Nanocellulose from Unbleached Hemp Fibers as a Filler for Biobased Photocured Composites with Epoxidized Cardanol

Journal of
Composites Science

MDPI

Article

Nanocellulose from Unbleached Hemp Fibers as a Filler for Biobased Photocured Composites with Epoxidized Cardanol

Sara Dalle Vacche [1,*], Vijayaletchumy Karunakaran [1,2], Silvia Maria Ronchetti [1], Alessandra Vitale [1] and Roberta Bongiovanni [1]

[1] Department of Applied Science and Technology, Politecnico di Torino, Corso Duca degli Abruzzi 24, 10129 Torino, Italy; vijayaletchumy13@s.unikl.edu.my (V.K.); silvia.ronchetti@polito.it (S.M.R.); alessandra.vitale@polito.it (A.V.); roberta.bongiovanni@polito.it (R.B.)

[2] Universiti Kuala Lumpur Malaysian Institute of Chemical and Bioengineering Technology (UniKL MICET), Lot 1988 Kawasan Perindustrian Bandar Vendor, Taboh Naning, Alor Gajah, Melaka 78000, Malaysia

* Correspondence: sara.dallevacche@polito.it; Tel.: +39-011-090-4565

Abstract: Biobased composites were successfully prepared using raw materials derived from biomass waste, i.e., an epoxy resin obtained from cardanol and nanocellulose from unbleached hemp fibers. The composites were prepared by solvent exchange and an impregnation of the cellulosic mat with the resin, followed by photocuring. Quantitative conversion was obtained, despite the high amount of fibers (30 wt%) and their absorbance in the UV region of the light spectrum. X-ray diffraction confirmed that the crystalline structure of cellulose did not change during the impregnation and curing process. The cured composites were flexible, hydrophobic, water resistant, transparent with a yellow/brown color, and in the rubbery state at room temperature.

Keywords: biobased polymers; photocuring; X-ray diffraction; Fourier-transform infrared spectroscopy; nanocellulose; hemp; epoxidized cardanol

Citation: Dalle Vacche, S.; Karunakaran, V.; Ronchetti, S.M.; Vitale, A.; Bongiovanni, R. Nanocellulose from Unbleached Hemp Fibers as a Filler for Biobased Photocured Composites with Epoxidized Cardanol. *J. Compos. Sci.* **2021**, *5*, 11. https://doi.org/10.3390/jcs5010011

Received: 3 December 2020
Accepted: 30 December 2020
Published: 3 January 2021

1. Introduction

As sustainability becomes an essential attribute of products and processes, the development of new materials obtained from renewable sources and with environmentally friendly processes is a current research goal. Low energy requirement, room temperature operation, and low release of volatile organic compounds (VOCs) make photoinduced polymerization a green technology that has the potential of becoming even greener due to new developments in the irradiation sources (e.g., visible light sources, halogen, fluorescence, and LED bulbs, sunlight) and photoinitiating systems, and due to the use of monomers from renewable and biobased sources [1–5]. Biobased composites, in which both the matrix and the filler are of a natural origin, are an interesting alternative due to their sustainability, especially if they are derived from secondary feedstock (nonedible biomass). Although they have not yet reach the performances of their petroleum-based counterparts, they are extensively researched for possible applications in fields where extreme performances are not needed, and sustainability is a key requirement in various areas, such as packaging and consumer goods, construction, and transportation [6,7]. In this regard, composites with cellulosic fillers, including nanocellulose, are very interesting due to the huge availability of cellulosic biomass.

Photocured composites with cellulosic fillers have been obtained with petroleum-based acrylate matrices: Water soluble polymers, such as poly(ethylene glycol) diacrylate and methacrylate modified polyvinyl alcohol, were used to obtain photocured hydrogels and aerogels [8–10]; in order to use as matrices polymers that are insoluble in water, e.g., photocurable hyperbranched acrylates, a solvent exchange process was proposed [11]. Recently, we demonstrated the possibility to photocure epoxidized cardanol in the presence of microfibrillated cellulose: the epoxy resin came from cashew nutshell liquid (CNSL),

which is a natural, non-food-chain, annually renewable biomaterial, while the reinforcing agent was from bleached wood fibers [12]. To make the material more compliant to the criteria of sustainability, the investigation in this work concerns composites where the nanocellulose is derived from hemp fibers obtained from agricultural waste. Hemp is a very sustainable annual plant, requiring low water and agrochemical input, and it can adapt to marginal lands or be used as a break crop to improve soil quality between cultures, thus not necessarily competing with or even improving the yield of edible crops [13]. Once cultivated mainly for textile fibers, hemp in Europe is presently grown as a multipurpose crop, as the aim is to use all parts of the plant, i.e., seeds, inflorescences, leaves, and stalks. The plants, when harvested at a later stage, provide shorter and lower quality bast fibers, separated from the stalk in an unaligned manner, thus unsuitable for textile applications; they are used in various ways (e.g., for paper pulp or insulation material), and high-added value applications are sought after [14]. In this work, the fibers were defibrillated by chemical and mechanical processes, but bleaching is avoided, as it usually requires harsh chemicals. The preparation of the composite was by a photoinduced process, coupled with an additional challenge of using a high content of fibers having a brownish color, thus absorbing light and reducing light penetration in the product.

2. Materials and Methods

2.1. Materials

The epoxidized cardanol (EC) resin NC-514S, with an epoxy equivalent weight of 418 g/mol, was provided by the Cardolite Corp. (Bristol, PA, US). For the photopolymerization, a cationic photoinitiator (PI), i.e., iodonium, (4-methylphenyl) [4-(2-methylpropyl) phenyl]-hexafluorophosphate(1-) diluted at 75% in propylene carbonate (Omnicat 250 by IGM Resins, Charlotte, NC, US), was used. The structures of EC and PI are shown in Figure 1.

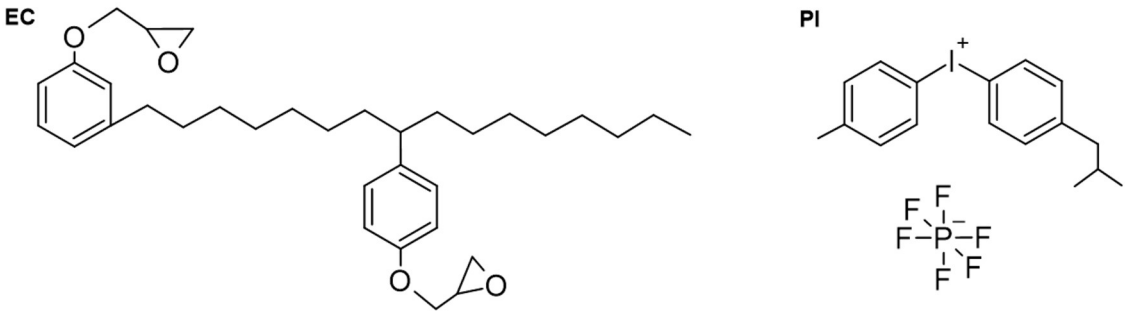

Figure 1. Structures of epoxidized cardanol (EC) NC-514S and of the cationic photoinitiator (PI).

The nanocellulose was obtained from unbleached hemp bast fibers, which were first chemically pretreated (10 wt% NaOH at room temperature for 2 h; 1M HCl at 80 °C for 1 h; 2 wt% NaOH at 80 °C for 1 h), then refined in a PFI beater (Metrotec SA, Lezo, Spain), treated with a cellulase enzyme, and finally defibrillated with a Supermasscolloider, an ultrafine friction grinder (Masuko Sangyo Co., Ltd., Saitama, Japan). The final product was in the form of an aqueous suspension with a solids content of 1.3 wt%, containing both individual rod-like fibrils with lengths of 100–300 nm and diameters of 5–12 nm, and stacks of nanofibrils with lengths of 380–3000 nm and widths between 20 and 200 nm, together with some larger fibers. A detailed account of the production and characterization of the nanocellulose will be reported in a separate publication.

For solvent exchange, acetone ≥99.5% by Sigma-Aldrich S.r.l. (Milano, Italy) was used.

2.2. Preparation of the Photocurable Resins and of the Composites

Photocurable resins were prepared by mixing the epoxidized cardanol (EC) with 10 or 15 wt% of the cationic photoinitiator (PI).

To prepare the composite films, the hemp nanocellulose suspension was filtered with a Büchner funnel connected to vacuum, fitted with a Durapore (Merck KGaA, Darmstadt,

Germany) membrane filter (hydrophilic PVDF, 47 mm diameter, 0.65 μm pore size). The nanocellulose wet mat formed on the filter was transferred to an acetone bath, allowing for the exchange of water with acetone. The acetone of the bath was refreshed 3 times over 24 h. Then, the pure acetone bath was replaced with the desired resin diluted at a 30 wt% concentration in acetone, and the impregnation of the mat was allowed to proceed for 2 h in the dark to prevent the advancement of the photocuring reaction. Finally, the impregnated mat was taken out from the bath, and the solvent was evaporated in a desiccator under vacuum for about 10 min at room temperature, which allowed us to obtain the uncured composites in the form of self-standing films with a thickness of about 180 μm.

For curing the composites, a 5000-EC UV flood lamp system (Dymax Corporation, Torrington, CT, USA) with a medium intensity mercury bulb (320–390 nm) was used. The intensity was fixed at 135 ± 5 mW/cm^2 by setting the distance between the specimen and the light source, and it was checked by means of a UV Power Puck II radiometer (EIT, LLC., Leesburg, VA, USA). The irradiation was carried out either in air or under a N_2 flux; the composites were turned upside down every minute to have homogeneous irradiation on the two sides; therefore, the irradiation time for the composites is indicated as $2 \times n$ minutes, where n is the number of minutes of irradiation per side.

In order to characterize the solvent exchanged cellulosic filler, some solvent exchanged nanocellulose mats were dried before the impregnation with the resin. The drying was carried out by slowly evaporating the remaining solvent at room temperature in a petri dish covered with its lid. Slow evaporation was needed in order to obtain transparent materials, as fast evaporation led to porous and opaque samples. The samples obtained in this way will be referred to as solvent-exchanged nanopaper, or simply nanopaper in what follows.

2.3. Characterization Methods

The UV-visible spectrum of the nanocellulose was collected with a JENWAY 6850 UV/Vis (Cole-Parmer, Stone, Staffordshire, UK) UV-visible spectrophotometer. The nanocellulose suspension, diluted to a 0.005 wt% concentration in demineralized water, was placed in a quartz cuvette, and an identical quartz cuvette filled with demineralized water was used as reference.

In order to follow the advancement of the curing reaction, the composites were analyzed by Fourier-transform infrared spectroscopy (FTIR) in attenuated total reflectance (ATR) mode using a Nicolet iS50 spectrometer (Thermo Fisher Scientific Inc., Waltham, MA, USA), equipped with an ATR accessory with a diamond crystal; the spectra were acquired in the 525–4000 cm^{-1} range, 32 scans per spectrum, and a resolution of 4 cm^{-1}. The degree of advancement of the curing reaction was calculated by the equation:

$$\eta = 1 - \frac{\frac{A(t)}{A^{ref}(t)}}{\frac{A(t=0)}{A^{ref}(t=0)}} \quad (1)$$

where A and A^{ref} are the areas of a peak corresponding to the epoxy group and to a reference peak, respectively, taken after an irradiation time t and before irradiation (t = 0).

The insoluble fraction of composite samples was determined gravimetrically to evaluate the weight loss of the specimens after immersion for 7 days in acetone.

Thermogravimetric analysis (TGA) was performed using a TGA/SDTA 851e instrument by Mettler Toledo (Greifensee, Switzerland). Scans were made from 25 to 800 °C with a heating rate of 20 °C min^{-1}, under a 60 mL min^{-1} flux of N_2, and the derivative thermogravimetric (DTG) curve (i.e., the first derivative of the weight vs temperature curve) was calculated in order to better resolve the main degradation events.

Differential scanning calorimetry (DSC) was carried out using a DSC1 STARe apparatus (Mettler Toledo, Greifensee, Switzerland). Two heating scans were performed on each sample, increasing the temperature range from −70 to 180 °C, at a rate of 10 °C min^{-1}, under a nitrogen flux.

X-ray diffraction characterization was performed on the solvent exchanged nanopaper and on the uncured and cured composites using a Panalytical X'Pert PRO (Panalytical, Almelo, The Netherlands) (Cu Kα radiation) diffractometer, with a PIXcel detector, a solid-state detector with rapid readout time and high dynamic range. Data collection has been performed at 40 kV and 40 mA, between 10° and 40° 2θ, with a step of 0.02° 2θ and a wavelength of 1.54187 Å.

3. Results

Composites were obtained impregnating hemp nanocellulose mats with photocurable resins containing the photoinitiator. The weight fraction of the hemp nanocellulose in the composites was calculated to be about 30 wt% from the quantity of nanocellulose suspension used for each mat and also from the resin uptake, estimated gravimetrically.

In a previous work [12], we found that while the resin could fully cure within minutes with the usual amounts of a photoinitiator (2–4 wt%), in the presence of microfibrillated cellulose from bleached wood fibers, the amount of photoinitiator and the radiation dose had to be increased due to secondary reactions: The superacid released by the photoinitiator upon irradiation promoted the acid hydrolysis of the cellulose chains and was thus not available for initiating the photocuring reaction. With a 5 wt% PI, the advancement of the curing reaction was negligible even with a high radiation dose, while a 15 wt% PI concentration eventually led to quantitative curing.

Adding to this challenge, the nanocellulose used in this work, obtained from unbleached fibers, absorbs light in the UV region (Figure 2), thus hindering its transmission through the material. Based on our previous results, in this work we selected 15 wt% as the upper limit for the PI concentration. We also tested a second PI concentration, intermediate to those tested in our previous work, i.e., 10 wt%, to check whether this could still lead to sufficient curing.

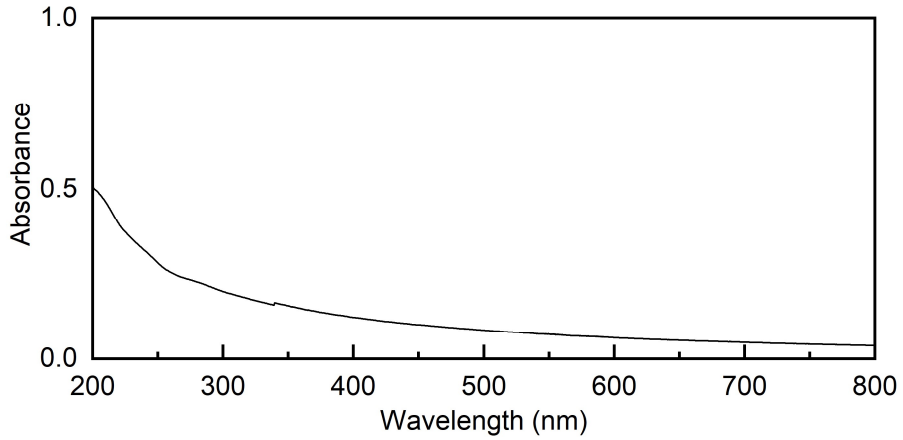

Figure 2. UV-visible spectrum of hemp nanocellulose (suspension in water at 0.005 wt%).

3.1. Photocuring of the Composites

As explained later in the text, the curing reaction could be initiated by light in the presence of 10 or 15 wt% in weight of the photoinitiator; only with the highest amount was the crosslinking of the matrix quantitative. Figure 3 reports the FTIR spectra of the composites with 15 wt% PI, uncured, and after different irradiation times. The spectrum of the solvent-exchanged nanopaper is also shown as a reference. The spectra of the composites with 10 wt% PI before and after irradiation are reported in Figure S1.

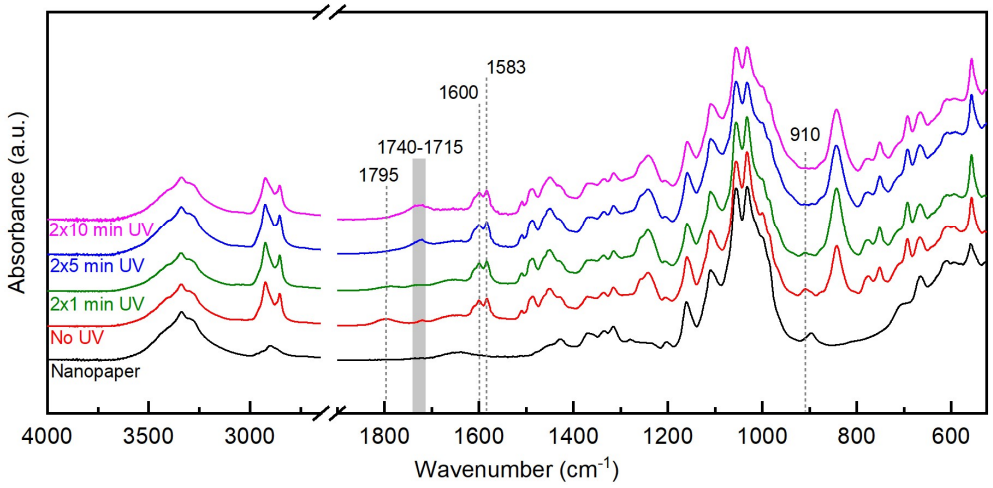

Figure 3. FTIR spectra of acetone exchanged dry nanocellulose (nanopaper) and of composites with 15 wt% PI, uncured (no UV) and cured for 2 × 1 min, 2 × 5 min, 2 × 10 min.

The spectrum of the nanopaper showed a broad band in the 3500–3100 cm^{-1} region due to the vibrations of O-H stretching of hydroxyl groups, characteristic bands in the 1300–1400 cm^{-1} region due to the vibrations of CH, CH_2, and CH_3 groups, and due to OH in plane bending, and in the 1100–950 cm^{-1} region corresponding to vibrations in cellulose alcohols, and a peak at 897 cm^{-1} corresponding to the symmetric ring stretching vibration of glycosidic bonds [15–18].

When the photocurable resin was added, the corresponding peaks appeared in the spectra of the composites [12]. The sp^3 C-H bond vibrations in the aliphatic chain of the epoxidized cardanol appeared at 2927 cm^{-1} and 2854 cm^{-1} [19–21], the vibrations of the C=C bonds in the aromatic rings at 1600 cm^{-1} and 1583 cm^{-1}, and those characteristic of the meta-substituted and para-substituted aromatic rings in the region below 900 cm^{-1}; the vibrations characteristic of the epoxide rings present in the epoxidized cardanol were located at 910 cm^{-1} [19,21–24], 860 cm^{-1} [20,21] and 776 cm^{-1} [21]. The main peaks characteristic of the photoinitiator were at 1795 cm^{-1}, corresponding to the vibration of the carbonyl group in the propylene carbonate solvent, and at 845 cm^{-1} belonging to the stretching vibrations of the hexafluorophosphate anion [12,25]. Due to superposition of the other peaks characteristic of the epoxide group with other signals, the evolution of the area of the peak at 910 cm^{-1} was followed in time to quantify the advancement of the reaction [12]. The area of the double peak at 1600 and 1583 cm^{-1} was taken as a reference. The degree of curing of the composites with 10 and 15 wt% PI are summarized in Table 1.

Table 1. Conversion calculated according to equation 1 for the composites with 10 and 15 wt% PI after irradiation for 5 min and 10 min per side; standard deviation is indicated in parenthesis.

Sample	Conversion (std. dev.)	
	2 × 5 min	**2 × 10 min**
10 wt% PI	0.38 (0.06)	0.40 (0.06)
15 wt% PI	0.87 (0.13)	0.95 (0.10)

A 10 wt% concentration of the photoinitiator proved not to be sufficient for leading the reaction to completion in the presence of the nanocellulose. Therefore, to obtain a quantitative conversion of the epoxy resin, the concentration of PI was increased to 15 wt%: Under these conditions, the peak at 910 cm^{-1} showed a significant intensity decrease with increasing exposure time, and eventually it disappeared, indicating that the ring-opening reaction reached quantitative conversion (Figure 3).

While, upon irradiation, the peak at 1795 cm^{-1} related to carbonyl groups in the PI decreased with exposure time, in the same region a new peak appeared, centered around 1725 cm^{-1}, attributed to the appearance of carbonyl groups due to autooxidation of the resin [12]. This effect was indeed significantly suppressed by irradiating the composites under a flux of nitrogen (see Figure S2).

3.2. Characterization of the Composites

Photos of the composites, uncured and irradiated for 5 min on each side (2 × 5 min), are shown in Figure 4. The composites, even after photocuring, were flexible and transparent. They showed a yellow/brown color that became darker upon curing. The color was both due to the hemp nanocellulose, which absorbs above 400 nm (Figure 3), and due to the resin. While the solvent-exchanged nanopaper instantly absorbed water and started to deform, the composites showed hydrophobic behavior and were water resistant (see Video S1).

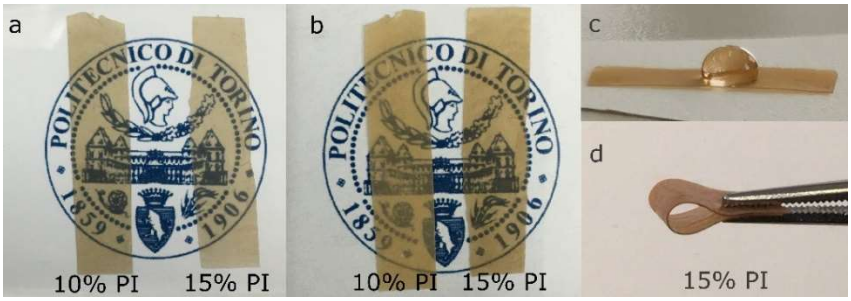

Figure 4. Composite of epoxidized cardanol and hemp nanocellulose with 10 and 15 wt% photoinitiator (PI): (**a**) before curing and (**b**) after curing for 5 min of on each side; (**c**) water drop on composite with 15 wt% PI cured for 5 min of on each side, and (**d**) photo showing the flexibility of the cured composite.

The FE-SEM observation of the surface of the composite with 15 wt% PI, irradiated for 2 × 5 min (Figure 5), showed a homogeneous distribution of the nanocellulose; the microstructure formed by the nanocellulose fibers could be clearly seen. Some small pores were visible, particularly in the vicinity of larger fibers.

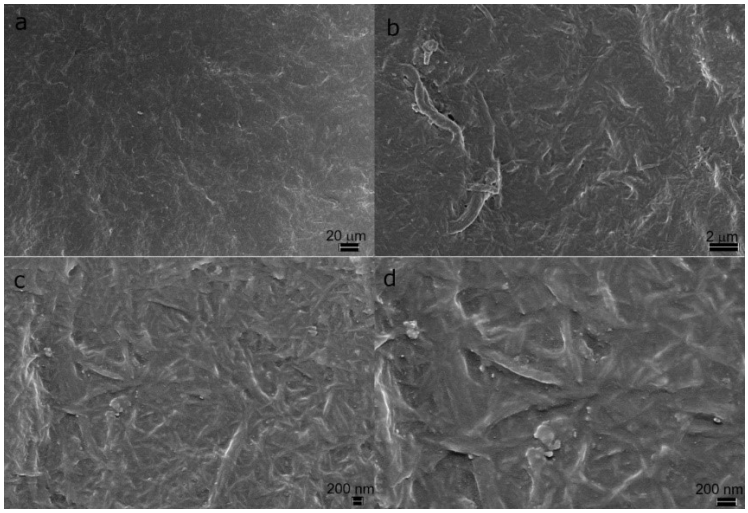

Figure 5. FE-SEM images of the surface of a composite with 15 wt% PI, irradiated for 5 min on each side, at increasing magnification: (**a**) shows a good macroscopic homogeneity of the surface; in (**b**) larger fibers, and pores in their vicinity, are visible; (**c**,**d**) show closer views of the surface of the composites evidencing the structure formed by the cellulose fibrils.

Samples of uncured composite and cured composite with 15 wt% PI (irradiated for 2 × 10 min) underwent an immersion of 7 days in acetone, in order for us to assess the insoluble content. The insoluble content for the uncured composite was 43 wt%, while for the cured composite it increased to 87 wt%, owing to the crosslinking of the resin. The FTIR analysis of the samples before and after the immersion in acetone is reported in Figure 6.

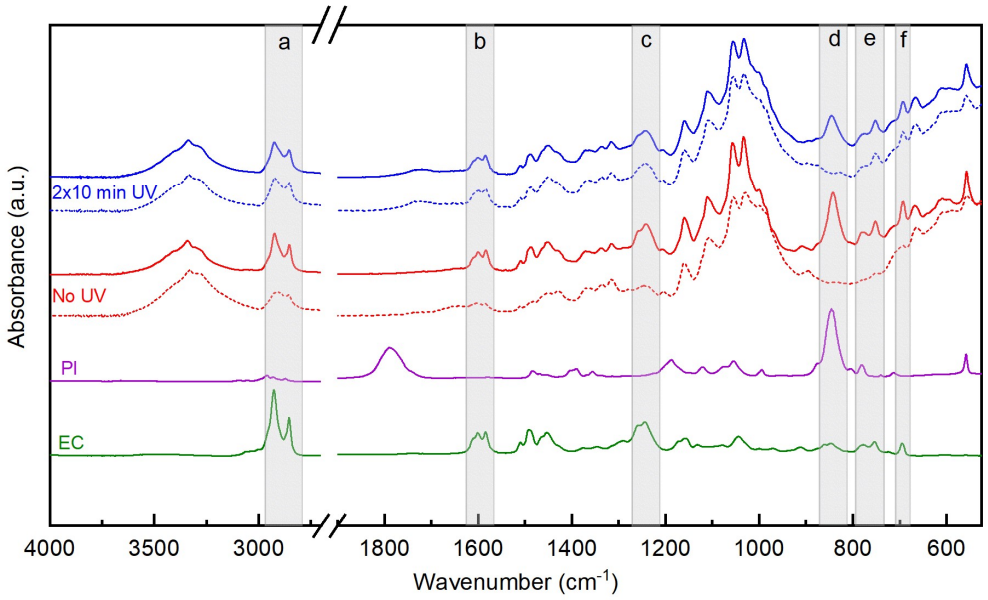

Figure 6. Spectra of samples of nanopaper and composite with 15 wt% PI, uncured (no UV) and cured (2 × 10 min UV) before (solid lines) and after removal of the soluble fraction (dashed lines). The grey areas indicate the regions of the spectra where differences were highlighted. Spectra of epoxidated cardanol (EC) and photoinitiator (PI) are shown as reference.

For the uncured composite, the intensity of the peaks associated to the resin (regions indicated as a–f in Figure 6) drastically decreased after immersion in acetone, indicating the removal of the epoxidized cardanol and of the photoinitiator. After the immersion test, peaks at 910 and 860 cm^{-1}, associated to epoxide ring vibrations, were not detected, indicating the absence of uncured resin. However, the peaks related to the aromatic and aliphatic groups of the resin were still visible after immersion, suggesting that actually a small amount of resin remained in the system after the test, and had cured even in the absence of UV irradiation, despite care being taken in keeping the sample in the dark as much as possible during preparation and handling. On the other hand, for the cured composite no changes were detected in the regions of a–c, e, f in Figure 6; only the peak at 845 cm^{-1} (in region d in Figure 6) disappeared. As no signal associated with the epoxide rings was visible for the cured composite at 910 cm^{-1} before immersion in acetone, and as all other peaks related to the epoxidated cardanol remained of similar intensity after the test, it is reasonable to assume that some free photoinitiator fragments, in particular the hexafluorophosphate counterion, remained in the cured composite and were then released during immersion in acetone.

In order to understand whether the process for fabricating the composites induced changes in the crystalline structure of the cellulose, an X-ray diffraction analysis was performed on the solvent-exchanged nanopaper and on the uncured and cured composites (Figure 7). The three main characteristic peaks (1-10), (110), and (200) of cellulose Iβ [26] were visible in all patterns, although the relative intensities of the peaks of the composites were different from those of the nanopaper. Furthermore, the patterns of composites showed a shoulder at about 20.5° that can be assigned to the (012) and (102) reflections of cellulose Iβ, confirming a random orientation of the crystallites [23]. Finally, a peak appeared in the diffractogram of the nanopaper at 12.2° 2θ, assigned to the $(1\bar{1}0)$ plane of cellulose II. The presence of a small amount of cellulose II may be due to the strong alkaline

treatment [27]. The difference in the relative intensity of the peaks between nanopaper and composites may be attributed to a different orientation of the crystalline planes, due to the swelling of the fiber network by the impregnation with resin. On the other hand, the patterns relative to the two composites can be superposed; the slight shift is attributed to alignment differences due to the non-perfect planarity of the samples.

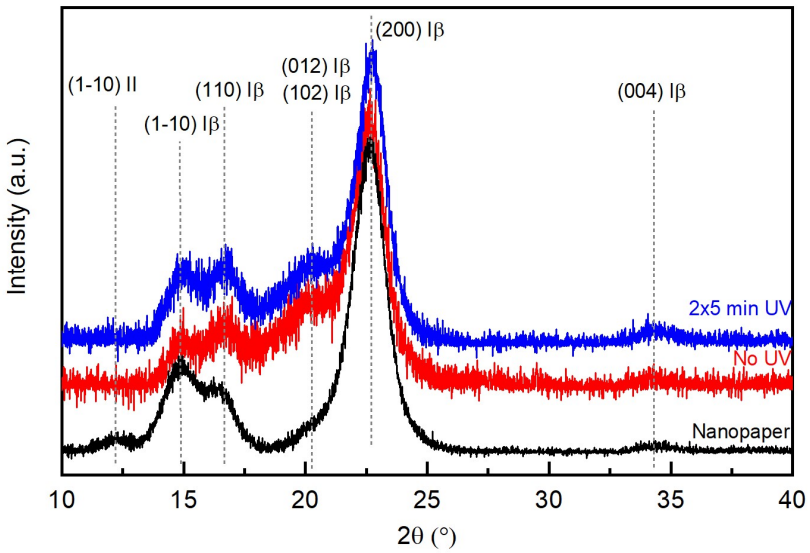

Figure 7. X-ray diffraction analysis.

The thermograms obtained by differential scanning calorimetry for the composites with 15 wt% PI, before and after UV irradiation, are reported in Figure 8. The uncured composite showed a step change in the heat flow associated with the glass transition temperature (T_g) at −46 °C in the first heating scan, and −43 °C in the second heating scan; for the cured composite, the T_g was detected around 1 °C in both heating scans. Furthermore, a broad endotherm transition, in the form of a double peak, was detected only in the first heating scan of both the cured and uncured composites, and it was associated with the evaporation of residual acetone and bound water.

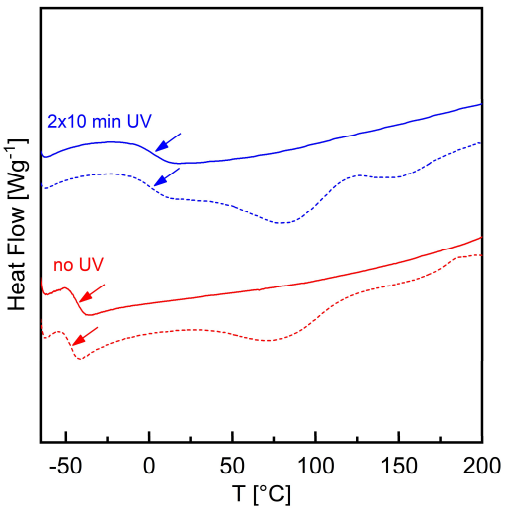

Figure 8. Differential scanning calorimetry: thermograms of composites with 15 wt% PI, uncured (no UV) and with 2 × 10 min of UV irradiation; first (dashed lines) and second (solid lines) heating scans.

The results of the thermogravimetric analysis performed on composites with 10 wt% and 15 wt% PI, before curing and after curing, are reported in Figure 9. The same figure

also reports as reference the weight loss curve and its first derivative (DTG) for solvent exchanged nanopaper, showing a one-step decomposition, with maximum degradation rate at 370 °C, and a residual weight equal to 17% of the initial one.

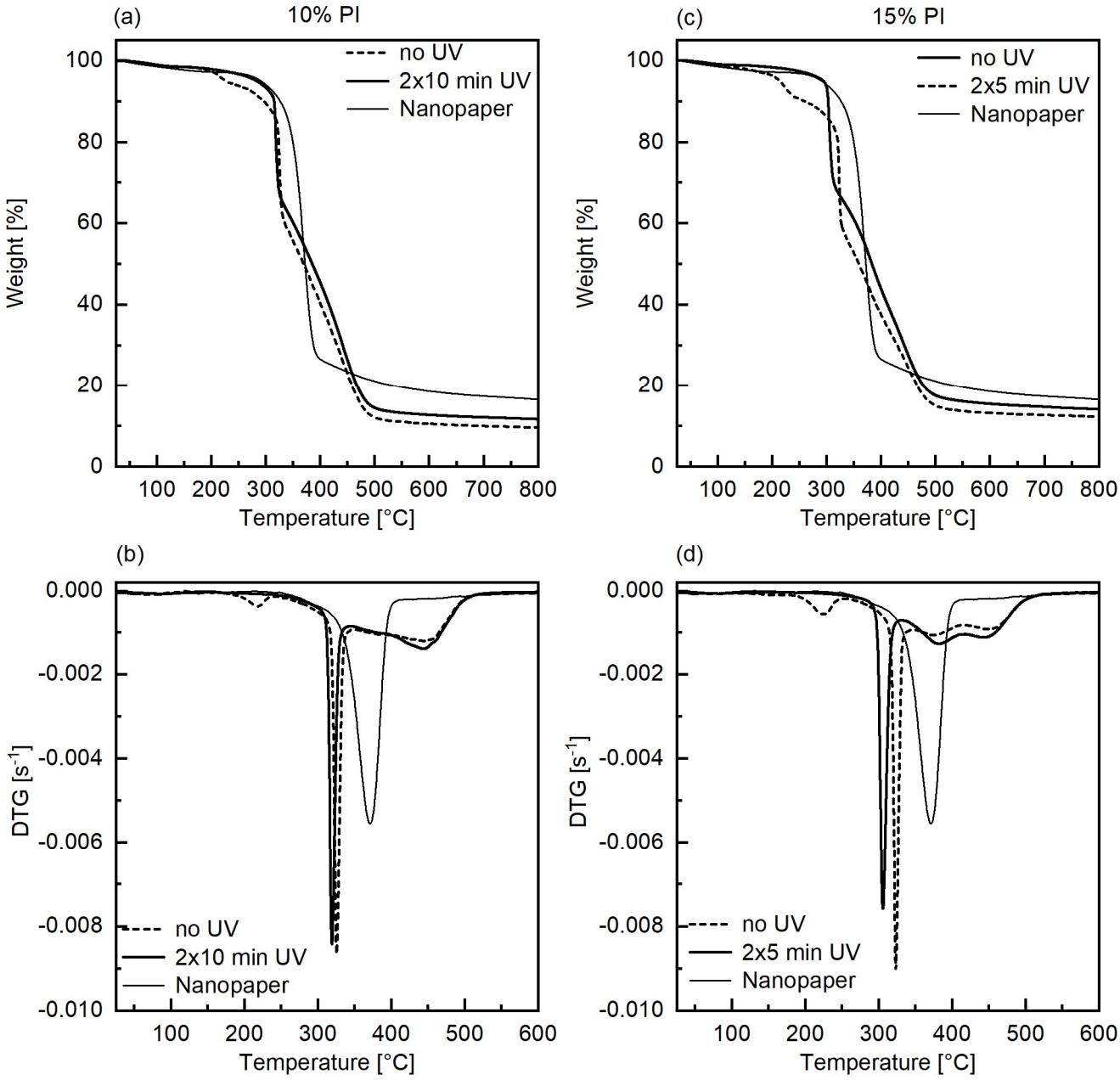

Figure 9. Thermogravimetric analysis (i.e., weight loss and derivative thermogravimetric curves (DTG)) of composites with 10 wt% PI (**a**) and (**b**), uncured (dashed line) and cured for 2 × 10 min (solid line), and with 15 wt% PI (**c**) and (**d**), uncured (dashed line) and cured for 2 × 5 min (solid line); results for the solvent exchanged nanopaper (thin lines) are reported in all graphs as reference.

For all composites, a small weight loss around 80 °C was present, confirming the loss of the solvent associated with the endotherm peak in the DSC analysis. For the uncured composites, a degradation event with an onset at 200 °C and a maximum degradation rate at 225 °C was related to the PI, and specifically to the evaporation of propylene carbonate; indeed, the integrated area of the DTG peak corresponded to about 2% and 3.5%, respectively, of the initial weights. This weight loss was not present after curing. Then, for the uncured composites, an abrupt step attributed to cellulose degradation was

present with a maximum degradation rate around 320 °C, representing about 30%–35% of the initial weight. Upon curing, the degradation temperature of cellulose decreased to 319 °C and 305 °C, for 10 and 15 wt% PI concentrations, respectively. The reduction of the degradation temperature of cellulose is consistent with the hypothesis of acid hydrolysis of cellulose caused by the release of superacid upon decomposition of the photoinitiator. Indeed, the degradation temperature of cellulose was higher for the composite with the lower amount of PI, indicating lower damaging of cellulose, despite a longer irradiation time. Finally, a gradual weight loss amounting to slightly less than 50% of the initial weight was present between 400 and 550 °C, which was attributed to the decomposition of the resin; this gradual weight loss was resolved in two peaks in the DTG curve. The decomposition of the resin took place in the same range of temperatures for both the uncured and cured composites: This suggests that during the thermal scan, the resin polymerizes as the onium salts can also thermally decompose [28]. The residual weight slightly increased about 2 percentage points for both the cured composites with respect to the corresponding uncured ones.

4. Conclusions

Nanocellulose obtained from unbleached hemp fibers was used as a filler for biobased composites with a commercial epoxidized cardanol resin. The fabrication process of the composite did not alter the crystalline structure of the nanocellulose. The composites were cured successfully with UV light in the presence of a cationic photoinitiator: The high load of fibers (30 wt%) and their absorbance in the UV range did not prevent achieving quantitative conversion. Composite nanopapers were fabricated: they were transparent, hydrophobic, water resistant, and with a brownish color; they were rubbery, with their glass transition being below room temperature, and flexible. Thus, an interesting material was obtained from cheap components derived from waste biomass.

Supplementary Materials: The following are available online at https://www.mdpi.com/2504-477X/5/1/11/s1, Figure S1: FTIR spectra of composites with 10 wt% PI, uncured (no UV) and cured for 2 × 1 min, 2 × 5 min, 2 × 10 min., Figure S2: FTIR spectra of composites with 15 wt% PI, irradiated under N_2 flux. Video S1: Deposition of a drop of water on the solvent exchanged nanopaper and on a cured composite: water is absorbed by the nanopaper, which is thus deformed, while it is not absorbed by the composite, which is not affected.

Author Contributions: Conceptualization, S.D.V. and R.B.; methodology, S.D.V., and A.V.; formal analysis, S.D.V. and S.M.R.; investigation, S.D.V., V.K., and S.M.R.; resources, S.D.V. and R.B.; data curation, S.D.V.; writing—original draft preparation, S.D.V.; writing—review and editing, S.D.V., R.B., S.M.R., V.K., and A.V.; visualization, S.D.V.; supervision, R.B.; project administration, S.D.V. and R.B.; funding acquisition, S.D.V. and R.B. All authors have read and agreed to the published version of the manuscript.

Funding: The project ComBIOsites has received funding from the European Union's Horizon 2020 research and innovation program under the Marie Skłodowska-Curie grant agreement No 789454.

Acknowledgments: The authors are grateful to Cardolite for donating the epoxidized cardanol resin, and to STIIMA-Biella, Consiglio Nazionale delle Ricerche (Italy), and LGP2, Grenoble INP-Pagora (France) for help with nanocellulose preparation. V.K. acknowledges the support of the Erasmus+ programme of the European Union.

Conflicts of Interest: The authors declare no conflict of interest. The funders had no role in the design of the study; in the collection, analyses, or interpretation of data; in the writing of the manuscript, or in the decision to publish the results.

References

1. Tehfe, M.; Louradour, F.; Lalevée, J.; Fouassier, J.-P. Photopolymerization Reactions: On the Way to a Green and Sustainable Chemistry. *Appl. Sci.* **2013**, *3*, 490–514. [CrossRef]
2. Lalevée, J.; Fouassier, J.P. Recent advances in sunlight induced polymerization: Role of new photoinitiating systems based on the silyl radical chemistry. *Polym. Chem.* **2011**, *2*, 1107. [CrossRef]

3. Tehfe, M.-A.; Lalevée, J.; Gigmes, D.; Fouassier, J.P. Green Chemistry: Sunlight-Induced Cationic Polymerization of Renewable Epoxy Monomers under Air. *Macromolecules* **2010**, *43*, 1364–1370. [CrossRef]
4. Molina-Gutiérrez, S.; Dalle Vacche, S.; Vitale, A.; Ladmiral, V.; Caillol, S.; Bongiovanni, R.; Lacroix-Desmazes, P. Photoinduced Polymerization of Eugenol-Derived Methacrylates. *Molecules* **2020**, *25*, 3444. [CrossRef]
5. Noè, C.; Malburet, S.; Bouvet-Marchand, A.; Graillot, A.; Loubat, C.; Sangermano, M. Cationic photopolymerization of bio-renewable epoxidized monomers. *Prog. Org. Coat.* **2019**, *133*, 131–138. [CrossRef]
6. Mohanty, A.K.; Vivekanandhan, S.; Pin, J.-M.; Misra, M. Composites from renewable and sustainable resources: Challenges and innovations. *Science* **2018**, *362*, 536–542. [CrossRef]
7. La Mantia, F.P.; Morreale, M. Green composites: A brief review. *Compos. Part A Appl. Sci. Manuf.* **2011**, *42*, 579–588. [CrossRef]
8. Bai, C.; Tang, A.; Zhao, S.; Liu, W. Flexible Nanocellulose/Poly(ethylene glycol) Diacrylate Hydrogels with Tunable Poisson's Ratios by Masking and Photocuring. *BioResources* **2020**, *15*, 3307–3319.
9. Tang, A.; Li, J.; Li, J.; Zhao, S.; Liu, W.; Liu, T.; Wang, J.; Liu, Y. Nanocellulose/PEGDA aerogel scaffolds with tunable modulus prepared by stereolithography for three-dimensional cell culture. *J. Biomater. Sci. Polym. Ed.* **2019**, *30*, 797–814. [CrossRef]
10. Zhang, J.; Liu, T.; Liu, Z.; Wang, Q. Facile fabrication of tough photocrosslinked polyvinyl alcohol hydrogels with cellulose nanofibrils reinforcement. *Polymer* **2019**, *173*, 103–109. [CrossRef]
11. Galland, S.; Leterrier, Y.; Nardi, T.; Plummer, C.J.G.; Månson, J.A.E.; Berglund, L.A. UV-cured cellulose nanofiber composites with moisture durable oxygen barrier properties. *J. Appl. Polym. Sci.* **2014**, *131*, 131. [CrossRef]
12. Dalle Vacche, S.; Vitale, A.; Bongiovanni, R. Photocuring of Epoxidized Cardanol for Biobased Composites with Microfibrillated Cellulose. *Molecules* **2019**, *24*, 3858. [CrossRef] [PubMed]
13. Angelini, L.G.; Tavarini, S.; Candilo, M.D. Performance of New and Traditional Fiber Hemp (*Cannabis sativa* L.) Cultivars for Novel Applications: Stem, Bark, and Core Yield and Chemical Composition. *J. Nat. Fibers* **2016**, *13*, 238–252. [CrossRef]
14. Tang, K.; Struik, P.C.; Yin, X.; Thouminot, C.; Bjelková, M.; Stramkale, V.; Amaducci, S. Comparing hemp (*Cannabis sativa* L.) cultivars for dual-purpose production under contrasting environments. *Ind. Crop. Prod.* **2016**, *87*, 33–44. [CrossRef]
15. Stevulova, N.; Cigasova, J.; Estokova, A.; Terpakova, E.; Geffert, A.; Kacik, F.; Singovszka, E.; Holub, M. Properties Characterization of Chemically Modified Hemp Hurds. *Materials* **2014**, *7*, 8131–8150. [CrossRef]
16. Cintrón, M.S.; Hinchliffe, D.J. FT-IR Examination of the Development of Secondary Cell Wall in Cotton Fibers. *Fibers* **2015**, *3*, 30–40. [CrossRef]
17. Abraham, R.; Wong, C.; Puri, M. Enrichment of Cellulosic Waste Hemp (*Cannabis sativa*) Hurd into Non-Toxic Microfibres. *Materials* **2016**, *9*, 562. [CrossRef]
18. Boukir, A.; Fellak, S.; Doumenq, P. Structural characterization of Argania spinosa Moroccan wooden artifacts during natural degradation progress using infrared spectroscopy (ATR-FTIR) and X-Ray diffraction (XRD). *Heliyon* **2019**, *5*, e02477. [CrossRef]
19. Hu, Y.; Shang, Q.; Wang, C.; Feng, G.; Liu, C.; Xu, F.; Zhou, Y. Renewable epoxidized cardanol-based acrylate as a reactive diluent for UV-curable resins. *Polym. Adv. Technol.* **2018**, *29*, 1852–1860. [CrossRef]
20. Cheon, J.; Cho, D.; Song, B.K.; Park, J.; Kim, B.; Lee, B.C. Thermogravimetric and Fourier-transform infrared analyses on the cure behavior of polycardanol containing epoxy groups cured by electron beam. *J. Appl. Polym. Sci.* **2015**, *132*, 132. [CrossRef]
21. Chen, J.; Nie, X.; Liu, Z.; Mi, Z.; Zhou, Y. Synthesis and Application of Polyepoxide Cardanol Glycidyl Ether as Biobased Polyepoxide Reactive Diluent for Epoxy Resin. *ACS Sustain. Chem. Eng.* **2015**, *3*, 1164–1171. [CrossRef]
22. Natarajan, M.; Murugavel, S.C. Thermal stability and thermal degradation kinetics of bio-based epoxy resins derived from cardanol by thermogravimetric analysis. *Polym. Bull.* **2017**, *74*, 3319–3340. [CrossRef]
23. Dworakowska, S.; Cornille, A.; Bogdał, D.; Boutevin, B.; Caillol, S. Formulation of bio-based epoxy foams from epoxidized cardanol and vegetable oil amine. *Eur. J. Lipid Sci. Technol.* **2015**, *117*, 1893–1902. [CrossRef]
24. Kanehashi, S.; Tamura, S.; Kato, K.; Honda, T.; Ogino, K.; Miyakoshi, T. Photopolymerization of Bio-Based Epoxy Prepolymers Derived from Cashew Nut Shell Liquid (CNSL). *JFST* **2017**, *73*, 210–221. [CrossRef]
25. Logacheva, N.M.; Baulin, V.E.; Tsivadze, A.Y.; Pyatova, E.N.; Ivanova, I.S.; Velikodny, Y.A.; Chernyshev, V.V. Ni(II), Co(II), Cu(II), Zn(II) and Na(I) complexes of a hybrid ligand 4′-(4‴-benzo-15-crown-5)-methyloxy-2,2′:6′,2″-terpyridine. *Dalton Trans.* **2009**, 2482–2489. [CrossRef]
26. French, A.D. Idealized powder diffraction patterns for cellulose polymorphs. *Cellulose* **2014**, *21*, 885–896. [CrossRef]
27. Dinand, E.; Vignon, M.; Chanzy, H.; Heux, L. Mercerization of primary wall cellulose and its implication for the conversion of cellulose I→cellulose II. *Cellulose* **2002**, *9*, 7–18. [CrossRef]
28. Sundell, P.-E.; Jönsson, S.; Hult, A. Thermally induced cationic polymerization of divinyl ethers using iodonium and sulfonium salts. *J. Polym. Sci. Part A Polym. Chem.* **1991**, *29*, 1535–1543. [CrossRef]